NUMERICAL STUDIES ON THE DYNAMIC BEHAVIOR OF A SUPERLONG CURVED PONTOON BRIDGE UNDER WIND AND WAVE ACTIONS

Conference Paper · January 2019

DOI: 10.7712/120119.7352.19214

3 authors:

Aksel Fenerci
Norwegian University of Science and Technology

Yuwang Xu
Norwegian University of Science and Technology

Ole Øiseth
Norwegian University of Science and Technology

Available online at www.eccomasproceedia.org
Eccomas Proceedia COMPDYN (2019) 5872-5879

ECCOMAS
Proceedia

COMPDYN 2019
7th ECCOMAS Thematic Conference on
Computational Methods in Structural Dynamics and Earthquake Engineering
M. Papadrakakis, M. Fragiadakis (eds.)
Crete, Greece, 24–26 June 2019

NUMERICAL STUDIES ON THE DYNAMIC BEHAVIOR OF A SUPER-LONG CURVED PONTOON BRIDGE UNDER WIND AND WAVE ACTIONS

Aksel Fenerci[1], Yuwang Xu[2] and Ole Øiseth[1]

[1] Norwegian University of Science and Technology, Department of Structural Engineering
Richard Birkelandsvei 1A 7034 Trondheim
e-mail: {aksel.fenerci,ole.oiseth}@ntnu.no

[2] School of Naval Architecture, Ocean & Civil Engineering, Shanghai Jiao Tong University
800 Dongchuan Road, Shanghai, China
xuyuwang@sjtu.edu.cn

Abstract

Floating bridges serve as attractive solutions where classical bridge concepts are not possible. However, compared to more commonly encountered bridge concepts such as cable-supported bridges, their dynamic behavior remains less investigated. Here, an end-supported pontoon bridge, currently under development by the Norwegian Public Roads Administration (NPRA) for the Bjørnafjord crossing in Norway, is considered as a case study to investigate its dynamic behavior under combined wind and wave loading. The stochastic dynamic behavior of the bridge are evaluated using state-of-the-art time domain analysis techniques. The frequency-dependent motion induced forces are modeled using state-space formulations, which are then embedded into the general-purpose finite element software ABAQUS, where the global dynamic analysis is carried out. Results of global response measures at the bridge girder are presented and the results are carefully discussed.

Keywords: floating bridge, buffeting, first-order waves, stochastic dynamics, radiation forces, self-excited forces, state-space model

doi: 10.7712/120119.7352.19214

1 INTRODUCTION

Although they are still relatively rare, floating bridges offer viable and economically efficient alternatives to the more classical long-span bridges. Span lengths so far has not been crossed with cable-supported bridges can possibly be crossed with floating bridges, without needing massive increase in the cost due to impractically large section dimensions. Such a solution for crossing the 5 km wide, Bjørnafjord in Norway is currently under evaluation of the Norwegian Public Roads Administration (Statens Vegvesen) as part of the Ferry Free E39 Coastal Highway Project [1]. In contrast to the cable-supported bridges, however, the dynamic behavior of such structures under environmental actions is far less investigated. The harsh nature of the Norwegian fjords together with its complex and mountainous topography in addition to the uniquely large scale of the structure makes such an evaluation increasingly challenging for the designing engineers. Significant efforts in understanding the underlying complex dynamics of the system are therefore necessary.

Dynamic analysis of floating bridges under random environmental loads require a stochastic dynamics approach, where the hydrodynamic effects at the pontoon locations and the aerodynamic interaction of the bridge girder with the wind should be modeled. Such an analysis can be carried out both in the frequency domain using spectral analysis [2,3] and in the time domain using Monte Carlo simulations [4,5]. Although significantly less time-efficient, time domain methods allow incorporation of the nonlinearities in the system. In a time domain approach, structural and geometric nonlinearities and nonlinear wind and wave forces can be included in the dynamic analysis, the effects of which might be important in case of such a slender structure. However, the frequency-dependent motion-induced forces, namely the aerodynamic self-excited forces and the hydrodynamic radiation forces that arise from the fluid-structure interaction, are more difficult to model in a time domain approach. For computational efficiency, radiation forces are conveniently modeled by state-space models [6,7] in analysis of large offshore structures and recently same approach was adopted for floating bridges [5]. Similar approaches can also be encountered in modeling of the self-excited forces in aerodynamic analysis of bridge decks [5,8,9].

Numerical simulations of the dynamic behavior of a super-long curved floating pontoon bridge under combined wind and wave actions are carried out in this study. The analysis is carried out in time domain, where the motion-induced forces are modeled using state-space models. The analysis results are presented in terms of standard deviations of the girder displacement and section forces.

Figure 1: Floating bridge crossing the Bjørnafjord

2 THE FLOATING BRIDGE CONCEPT

The floating bridge concept studied here is currently under concept development phase and considered a viable option for crossing the Bjørnafjord in Norway, which is a 5 km wide fjord in Hordaland, Norway. The fjord is exposed to strong winds and waves from the Norwegian Sea and the depth of the seabed does not allow for abutments, which would support a classical bridge. Therefore, a floating bridge with that is supported by pontoons is considered for the crossing (Figure 1). The proposed bridge consists of mainly three parts: a cable-stayed bridge that would allow the passage of ships underneath it, a high-bridge part that provides the transition between the cable-stayed bridge and the pontoon bridge, and the low bridge that sits on floating pontoons (Figure 2). On top of each pontoon, columns support the bridge girder, which has a streamlined girder of 31 meters wide and 3.5 meters deep. The bridge is also curved, providing an arching effect against the harsh environmental loading from the open-sea exposure.

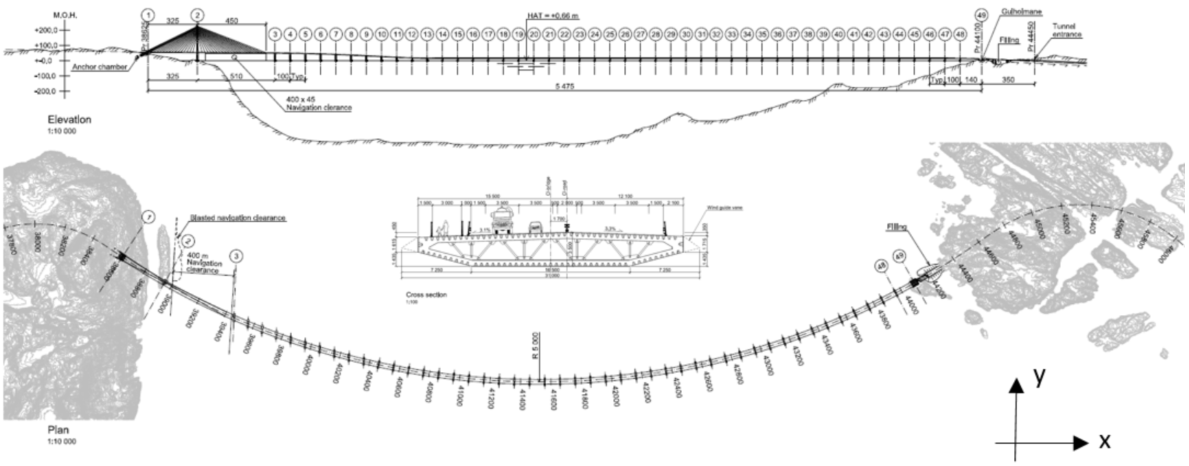

Figure 2: Technical Drawings (courtesy of Norwegian Public Roads Administration)

3 MODELING FRAMEWORK

In the framework of finite element discretization, the equation of motion of the structure under wind and wave loading, including the fluid-structure interaction terms, can be written as [5,7]

$$\mathbf{M}_s\ddot{\mathbf{u}}(t)+\mathbf{C}_s\dot{\mathbf{u}}(t)+(\mathbf{K}_s+\mathbf{K}_h)\mathbf{u}(t)=\mathbf{F}_{wind}+\mathbf{F}_{buff}(t)+\mathbf{F}_{se}(t)+\mathbf{F}_{wave}(t)-\mathbf{F}_{rad}(t) \quad (1)$$

where $\mathbf{M}_s$, $\mathbf{K}_s$, $\mathbf{C}_s$ are the structural mass, stiffness and damping matrices, $\mathbf{K}_h$ is the hydrostatic restoring stiffness matrix and $\mathbf{u}(t)$ is the vector of displacements. $\mathbf{F}_{wind}$ is the static wind load vector, $\mathbf{F}_{buff}(t)$ is the buffeting load vector and $\mathbf{F}_{wave}(t)$ is the first order wave load vector. $\mathbf{F}_{se}(t)$ and $\mathbf{F}_{rad}(t)$ denote the aerodynamic self-excited forces and the hydrodynamic radiation forces, respectively. The structural matrices are easily obtained using a finite element model of the structure (Figure 3), where the frequency-independent hydrostatic stiffness matrix can be obtained based on the buoyancy.

3.1 Motion-induced forces

The frequency-dependent motion-induced forces, $\mathbf{F}_{se}(t)$ and $\mathbf{F}_{rad}(t)$ will be modeled by state-space models for computational efficiency. The state-space model adopted for both terms can be written as

$$\begin{aligned}\dot{\mathbf{X}}(t) &= \mathbf{D}\mathbf{X}(t)+\mathbf{E}\mathbf{u}(t)\\ \mathbf{z}(t) &= \mathbf{Q}\mathbf{X}(t)\end{aligned} \tag{2}$$

where **X**(t) is the so-called state vector and **D, E, Q** are matrices of the model, $\mathbf{z}(t)$ denotes the frequency dependent part of the force vector. The system of equations given in the model gives a linear, continuous and time invariant system that describes the relationship between the motion of the structure and the motion-induced forces. The composition of the **D, E, Q** matrices depend on the functional form assumed to represent the forces. The detailed formulation of the models can be found in [5,10].

3.2 Buffeting and first-order wave forces

The buffeting forces due to wind turbulence and the wave forces are stochastic dynamic forces acting on the structure at pontoon locations and along the girder. They can be modeled as time-dependent nodal forces in the finite element framework described. However, the stochastic processes are generally defined in the form of spectral density matrices and Monte Carlo simulations are needed to obtain representative time-series of the processes.

Neglecting the aerodynamic admittance terms, the buffeting load vector for a girder node can be written assuming three degrees-of-freedom associated with the drag, lift and pitch motions of the girder as

$$F_{buff}(x,t)=\frac{\rho UB}{2}\begin{bmatrix}2(D/B) & (D/B)C_D{}'-C_L{}'\\ 2C_L & C_L{}'+(D/B)C_D{}'\\ 2BC_M & BC_M{}'\end{bmatrix}\begin{bmatrix}u(x,t)\\ w(x,t)\end{bmatrix} \tag{3}$$

where ρ is the air density, U is the mean wind velocity and B is the width of the bridge deck. C_D, C_L and C_M are the aerodynamic static coefficients of the bridge deck. Lastly, $u(x,t)$ and $w(x,t)$ are the time-series of the along-wind and vertical turbulences.

Similarly, the first-order wave forces exerted upon pontoons by the incident waves, this time acting on a node with six degrees of freedom, can be written as

$$\begin{aligned}&F_{wave}(x,y,t)=\sum_n\sum_m\left|\mathbf{T}(\omega_n,\theta_m)\right|\eta_{nm}\cos\left(k_n(x\cos(\theta_m)+y\cos(\theta_m)-\omega_n t+\varepsilon_{mn}-\phi_{mn}\right),\ n,m=\{1,2,...6\}\\ &\eta_{nm}=\sqrt{2S_\eta(\omega_n,\theta_n)\Delta\omega\Delta\theta},\ \phi_{mn}=\tan^{-1}\left(\frac{\mathrm{Im}\left(\mathbf{T}(\omega_n,\theta_m)\right)}{\mathrm{Re}\left(\mathbf{T}(\omega_n,\theta_m)\right)}\right)\end{aligned} \tag{4}$$

where ω, θ, η and k denote the frequency, direction, wave amplitude and wave number, respectively and $\mathbf{T}$ is the transfer function, which can be obtained via potential theory.

4 NUMERICAL SIMULATIONS

A detailed finite element model of the bridge, which was created in the general-purpose commercial finite element software ABAQUS [11] was supplied by the Norwegian Public Roads administration. The model (Figure 3) consists of beam elements representing the bridge girder and the columns and nodes at the water level at the pontoon locations. At the pontoon nodes, structural springs are used to model the hydrostatic stiffness of the pontoons. Prior to modal and dynamic analyses, the static loading on the structure, namely the prestressing of the cables, self-weight of the structure and the static wind loads are applied to get the correct stiffness. Eigenvalue analysis is carried out after the application of static loads. The first four mode shapes, along with the corresponding natural frequencies are shown in Figure 4. The first natural period of the structure is found to be around 116 seconds.

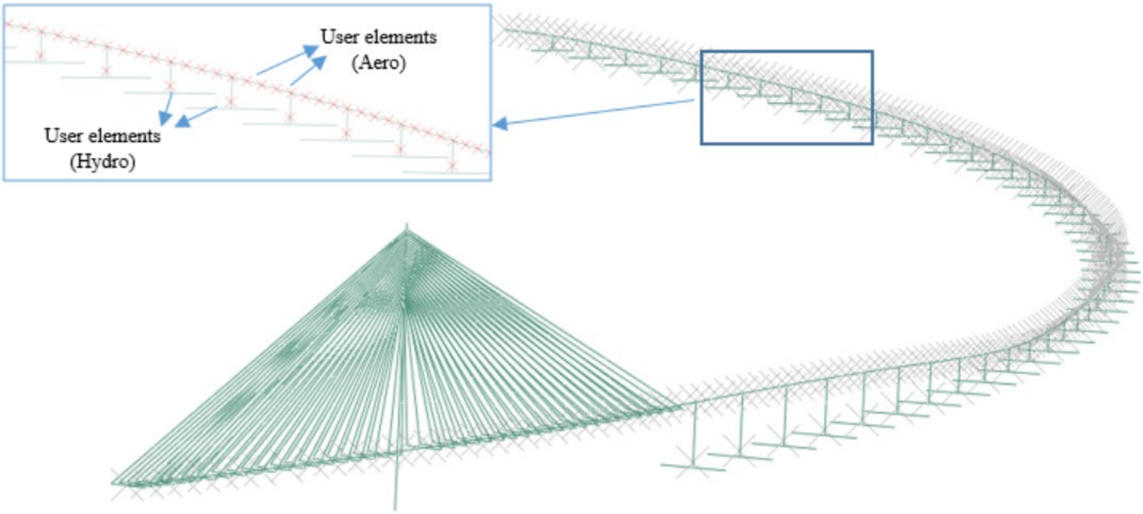

Figure 3: Finite element model of the bridge with aero and hydro user elements

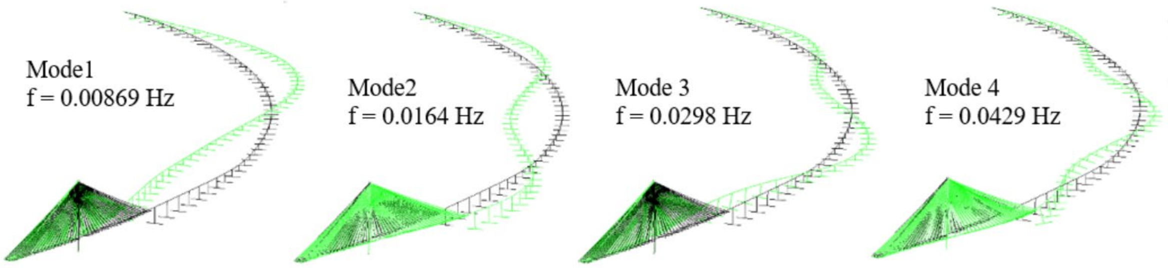

Figure 4: First four mode shapes and natural frequencies

4.1 Stochastic dynamic analysis

As discussed earlier, the definition of the stochastic environmental loads in the finite element model requires simulation of random time series from the processes defined by spectral characteristics. Time series of wind and wave forces are generated using an FFT-based simulation scheme [12]. The spectral densities of the processes are taken according to the design guidelines and the forms and parameters of the spectra are presented in Table 1. A Kaimal type of spectra along with Davenport coherence scheme is assumed for the wind turbulence, where the Jonswap spectrum along with a cos-2s directional distribution is adopted for the wave spectrum.

<table>
<tr><th>Wind spectra</th><th colspan="6">parameters</th></tr>
<tr><td rowspan="5">$$\frac{S_i f}{\sigma_i^2} = \frac{A_i f_z}{\left(1+1.5A_i f_z\right)^{5/3}},\ f_z = \frac{fz}{U},\ i = u,w$$
$$\frac{S_{nm}(f)}{\sqrt{S_n(f)S_m(f)}} = C = \exp(-K\frac{f.\Delta\mathrm{x}}{U}),\ m,n = \{u,w\}$$</td><td>U</td><td>30 m/s</td><td>C_{wy}</td><td>6.5</td><td>$C_D(C_D')$</td><td>0.53(0)</td></tr>
<tr><td>A_u</td><td>6.8</td><td>C_{wz}</td><td>3</td><td>$C_L(C_L')$</td><td>0.133(4.87)</td></tr>
<tr><td>A_w</td><td>9.4</td><td>I_u</td><td>0.14</td><td>$C_M(C_M')$</td><td>0.042(0.056)</td></tr>
<tr><td>C_{uy}</td><td>10</td><td>I_w</td><td>0.077</td><td></td><td></td></tr>
<tr><td>C_{uz}</td><td>10</td><td></td><td></td><td></td><td></td></tr>
<tr><th>Wave spectra</th><th colspan="6">parameters</th></tr>
<tr><td rowspan="3">$$S(\omega) = \frac{5H_s\omega_p^{\ 4}\left(1-0.278\ln(\gamma)\right)}{16\omega_p}\exp\left(-1.25\frac{\omega_p^{\ 4}}{\omega^4}\right)\gamma^{\exp\left(-\frac{(\omega-\omega_p)^2}{2\sigma^2\omega_p^{\ 2}}\right)}$$
$$\sigma = \begin{Bmatrix} 0.07 & for\ \ \omega \le \omega_p \\ 0.09 & for\ \ \omega > \omega_p \end{Bmatrix},\ \ \omega_p = 2\pi / T_p$$
$$D(\theta) = \cos^{2s}\left(\frac{\theta}{2}\right)$$</td><td colspan="2">s</td><td colspan="4">3</td></tr>
<tr><td colspan="2">Hs</td><td colspan="4">2.4</td></tr>
<tr><td colspan="2">Tp</td><td colspan="4">5.9</td></tr>
</table>

Table 1: Analysis input

The self-excited forces are modeled using the state-space model described in Eqn (2). The self-excited forces obtained by the quasi-steady theory are curve fitted by rational functions and the obtained coefficients are used to deduce the aerodynamic state-space model. Similarly, the hydrodynamic added mass and damping obtained from potential flow analyses in WADAM software using a panel model of the pontoon. The coefficients, which are obtained only at discrete frequencies, are then curve fitted using the method developed in [13]. The results of the curve fitting are then used to deduce the hydrodynamic state-space model.

The state-space models cannot be directly incorporated into the commercial finite element software. To overcome this obstacle, additional node elements at the existing nodes of the finite element model, defined by a user subroutine are introduced into the model, following the work of [5], where details of the implementation can be found.

5 ANALYSIS RESULTS

Dynamic analysis of the bridge is carried in time domain using the ABAQUS model, including the aerodynamic and hydrodynamic effects. 5 simulations of 1-hour duration each have been performed. The global responses along the length of the bridge girder, namely the strong and weak axis bending moments, the axial force and the displacements in three degrees-of-freedom (drag, lift and pitch) are extracted by post-processing the analysis results. The standard deviations of the global responses are then calculated using the hour-long signals at each node or integration point along the girder. The resulting standard deviations of the responses are plotted in Figure 5 for each simulation, where the average of five simulations is also shown.

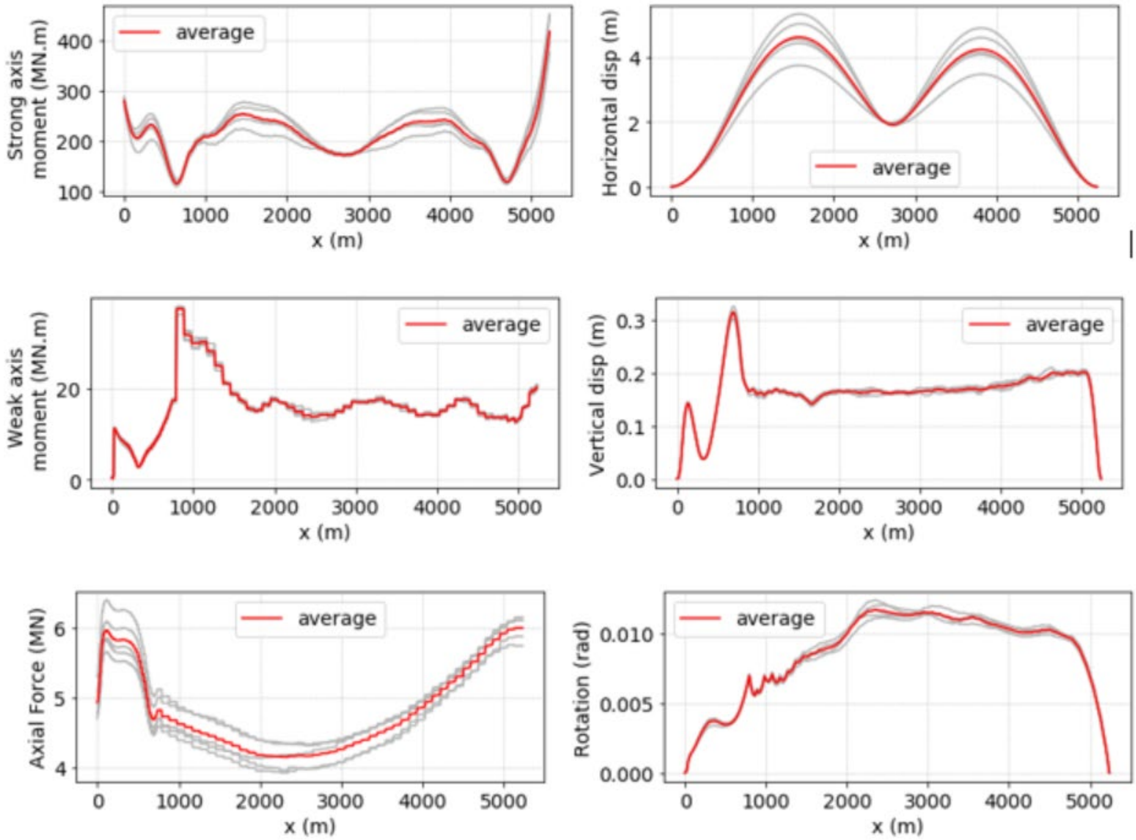

Figure 5: Standard deviations of the global responses of the bridge girder: the gray lines show different simulations, where the red lines are the averaged results

6 CONCLUSIONS

Dynamic behavior of a super-long curved pontoon bridge crossing the Bjørnafjord in Norway is investigated in this study under wind and wave loading. The analysis methodology is described and selected global responses under a certain environmental condition are presented.

Although the time-domain method discussed here has been used and verified against well-established frequency domain analyses before [5,10], comparisons are still necessary to ensure reliability of the approach. Such an analysis framework allows inclusion of also nonlinear phenomena with reasonable cost of computation, and opens possibilities for many investigations concerning the dynamic behavior of the structure. The contributions of wind and wave loadings and their interaction, different sources of damping, hydrodynamic interaction of the pontoons and global parametric stability of the entire bridge can be listed among others.

7 ACKNOWLEDGEMENTS

The research described here is financially supported by the Norwegian Public Roads Administration.

REFERENCES

[1] Dunham KK. Coastal Highway Route E39 - Extreme Crossings. Transp. Res. Procedia, vol. 14, 2016, p. 494–8. doi:10.1016/j.trpro.2016.05.102.

[2] Wirsching PH, Paez TL, Ortiz K. Random Vibrations: Theory and Practice. Dover Publications; 2006.

[3] Kvåle KA, Sigbjörnsson R, Øiseth O. Modelling the stochastic dynamic behaviour of a pontoon bridge: A case study. Comput Struct 2016;165:123–35. doi:10.1016/j.compstruc.2015.12.009.

[4] Shinozuka M. Monte Carlo solution of structural dynamics. Comput Struct 1972;2:855–74. doi:10.1016/0045-7949(72)90043-0.

[5] Xu Y, Øiseth O, Moan T. Time domain simulations of wind- and wave-induced load effects on a three-span suspension bridge with two floating pylons. Mar Struct 2018. doi:10.1016/j.marstruc.2017.11.012.

[6] Taghipour R, Perez T, Moan T. Hybrid frequency-time domain models for dynamic response analysis of marine structures. Ocean Eng 2008;35:685–705. doi:10.1016/j.oceaneng.2007.11.002.

[7] Naess A, Moan T. Stochastic Dynamics of Marine Structures. Cambridge: Cambridge University Press; 2012. doi:DOI: 10.1017/CBO9781139021364.

[8] Øiseth O, Rönnquist A, Sigbjörnsson R. Finite element formulation of the self-excited forces for time-domain assessment of wind-induced dynamic response and flutter stability limit of cable-supported bridges. Finite Elem Anal Des 2012;50:173–83. doi:10.1016/j.finel.2011.09.008.

[9] Xu Y, Øiseth O, Naess A, Moan T. Prediction of long-term extreme load effects due to wind for cable-supported bridges using time-domain simulations. Eng Struct 2017;148:239–53. doi:10.1016/j.engstruct.2017.06.051.

[10] Øiseth O, Rönnquist A, Sigbjörnsson R. Time domain modeling of self-excited aerodynamic forces for cable-supported bridges: A comparative study. Comput Struct 2011;89:1306–22. doi:10.1016/j.compstruc.2011.03.017.

[11] Dassault Systèmes Simulia, Fallis A., Techniques D. ABAQUS documentation. Abaqus 612 2013;53:1689–99. doi:10.1017/CBO9781107415324.004.

[12] Shinozuka M, Jan C-M. Digital simulation of random processes and its applications. J Sound Vib 1972;25:111–28. doi:10.1016/0022-460X(72)90600-1.

[13] Perez T, Fossen TI. A Matlab Toolbox for Parametric Identification of Radiation-Force Models of Ships and Offshore Structures. Model Identif Control A Nor Res Bull 2009;30:1–15. doi:10.4173/mic.2009.1.1.